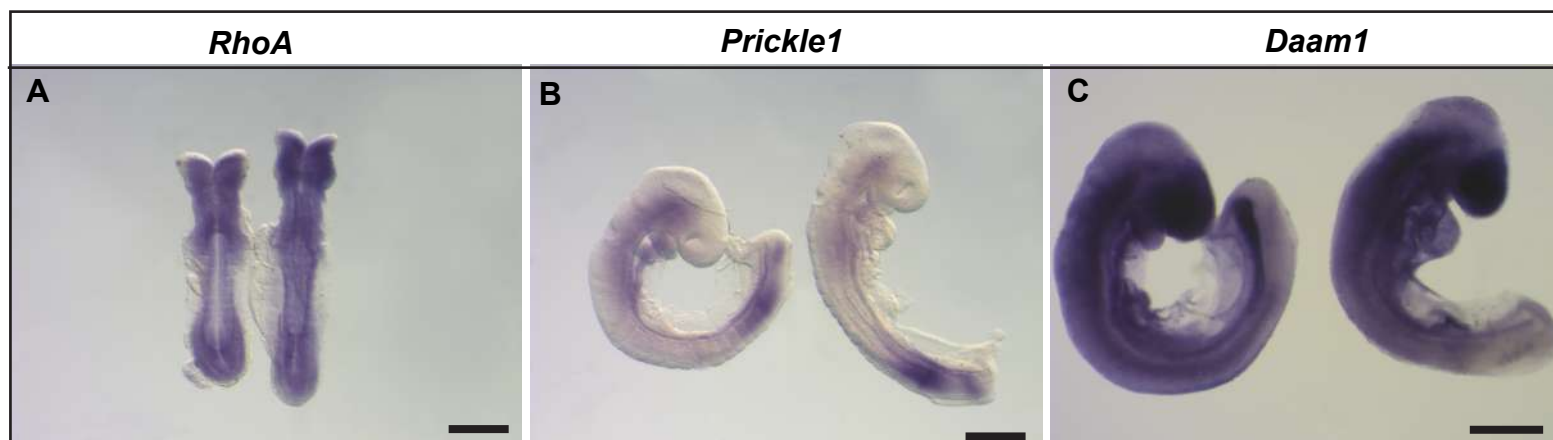


Figure S1



D

Gene	Fold change
<i>Wnt5a</i>	1.10
<i>Glypican4</i>	1.13
<i>PTK7</i>	1.17
<i>Daam1</i>	0.69
<i>Shroom3</i>	0.61
<i>F-actin</i>	0.66
<i>Myosin II-B</i>	1.14
<i>RhoA</i>	0.79
<i>Prickle1</i>	1.27

Figure S1: Expression of mRNA encoding genes in the Wnt-PCP pathway in *Vangl2*^{+/+} and *Vangl2*^{+/Lp} embryos. (A-C) *In situ* hybridisation of whole E9 mouse embryos *Vangl2*^{+/+} (left) and *Vangl2*^{+/Lp} (right) for: (A) *RhoA*; (B) *Prickle1*; (C) *Daam1*. (D) RT-PCR data presented as the fold change in gene expression, obtained by using the comparative C_T method. Scale bars in (A, B and C) = 500µm.

Figure S2

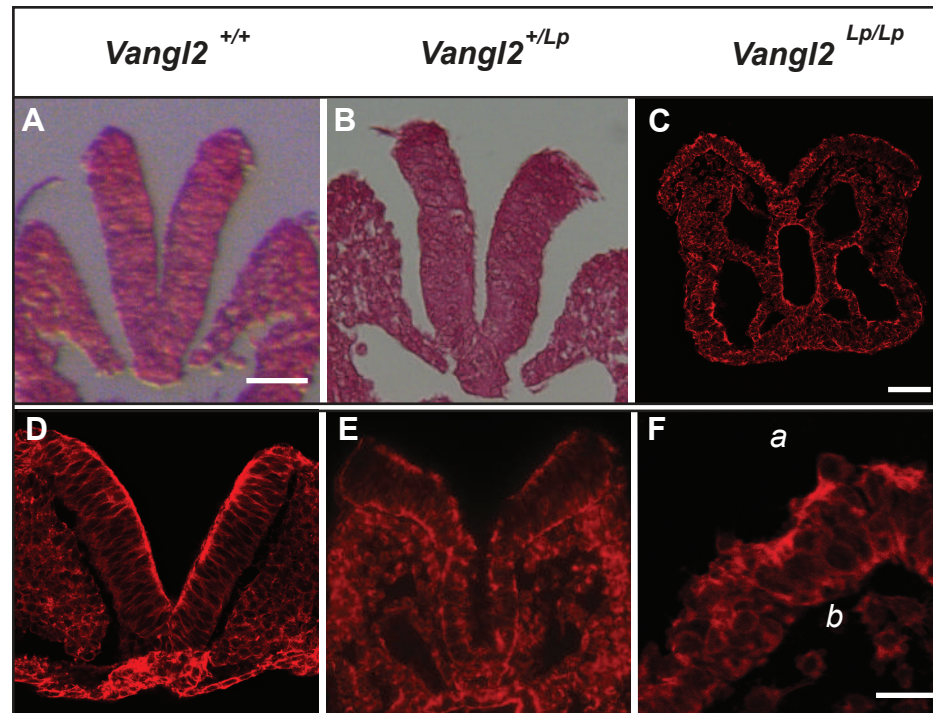


Figure S2: Disruption of neural fold morphology and apical actin distribution in E8.5 $Vangl2^{+/Lp}$ and $Vangl2^{Lp/Lp}$ embryos. Transverse sections of the PNP in: E8.5 $Vangl2^{+/+}$ (A and D) or $Vangl2^{+/Lp}$ (B and E) embryos. Transverse sections of the caudal region of an E9.5 $Vangl2^{Lp/Lp}$ embryo (C and F). (A and B) H&E staining and (C, D, E and F) phalloidin labelling: *a* and *b* in panel F represent the apical and basal side of the neural fold, respectively. Scale bars: (A) 50 μm , also for B, D and E; (C) 100 μm ; (F) 25 μm .

Figure S3

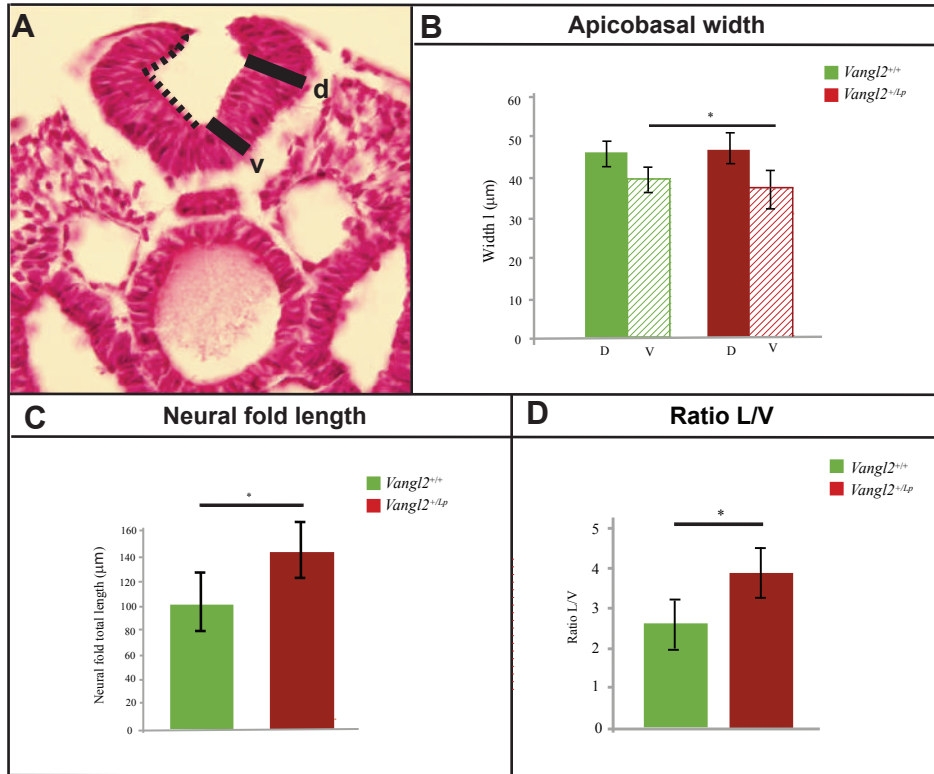


Figure S3: Variation in the apico-basal width and length of the neural folds. (A) Transverse section of *Vangl2*^{+/+} PNP showing the level of dorsal (*d*) and ventral (*v*) apico-basal widths of the straight portion of the neural fold juxtaposed to the paraxial mesoderm where the measurements were taken by the tracing line function in ImageJ. (B) Graph of the apico-basal width (in µm) at *d* and *v* of the straight portion of the neural plate in *Vangl2*^{+/+} and *Vangl2*^{+/Lp} embryos. (C) Graph representing the length (in µm) of the neural fold, measurements were taken with the tracing line function in ImageJ along the apical side, as shown in (A) by a dotted line. (D) The graph shows the ratio between the length (L) and the apico-basal ventral width (*v*) of the neural fold: (*): significant difference between *Vangl2*^{+/+} and *Vangl2*^{+/Lp} embryos, $p < 0.05$.

Figure S4

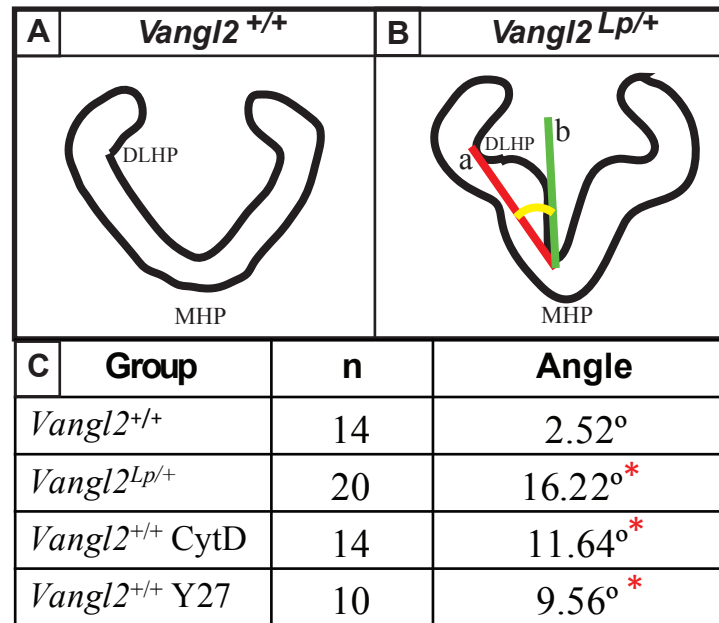


Figure S4: Bending and apical surface eversion of the neural folds. Diagram of a transverse section of the PNP from a *Vangl2*^{+/+} (A) and a *Vangl2*^{+Lp} embryo (B). The angles were taken from the line that joins the lumen side of the MHP and the DLHP (red line in B, a) and the line that joins the lumen side of the MHP and the most outward flexure point of the neural fold (green line in B, b). (C) The table shows the degree of eversion (angle) of the neural folds for each condition (group): n=number of neural folds analysed; MHP, Medial hinge point; DLHP, dorsolateral hinge point; red asterisk indicates significant difference from the *Vangl2*^{+Lp} embryos, the *Vangl2*^{+/+} embryos treated with CytD and the *Vangl2*^{+/+} embryos treated with Y-27632 compared to the *Vangl2*^{+/+} ($p < 0.05$).

Figure S5

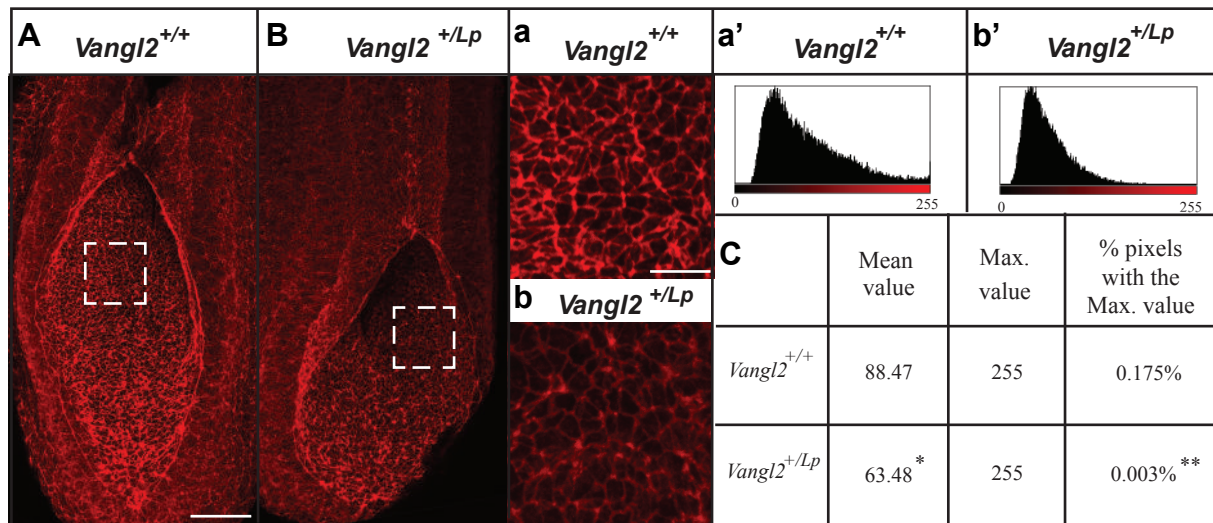


Figure S5: Quantification analysis of apical actin deposition. (A and B) Dorsal view of the maximum projection of the PNP from a *Vangl2*^{+/+} (A) and *Vangl2*^{+/Lp} embryo (B) labelled with phalloidin. (a and b) Magnified images (200 x 200 pixels) of the insets in A and B, respectively. The panels a' and b' represent the intensity histograms of phalloidin labelling from the areas in (a and b), respectively. (C) Table summarizing the data from the homologous histograms obtained from 3 *Vangl2*^{+/+} and 5 *Vangl2*^{+/Lp} embryos: "Mean value", average phalloidin intensity; "Max. value" maximum intensity obtained in the histogram; and "% pixels with the Max. value", the percentage of pixels with the maximum intensity. The difference between *Vangl2*^{+/+} and *Vangl2*^{+/Lp} embryos were statistical significant (* $p < 0.001$). Scale bars: (A) 50 μm also applies to B; (a) 12.5 μm also applies to b.

Figure S6

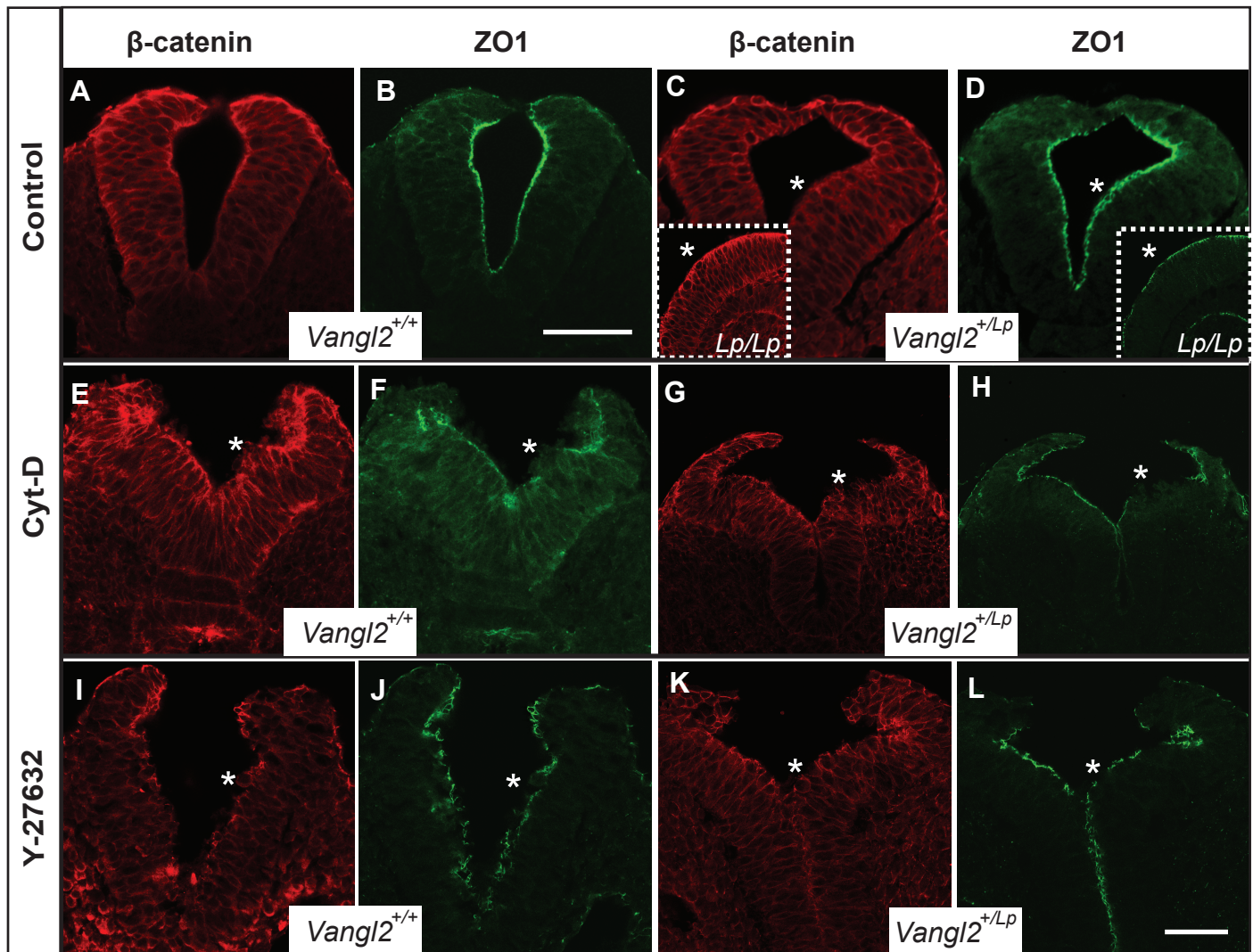


Figure S6: Disturbed apico-basal polarity in *Vangl2*^{+/*Lp*}, *Vangl2*^{*Lp/Lp*}, CytD and Y-27632 treated embryos. (A, B, E, F I and J) Transverse sections of *Vangl2*^{+/+} (C, D, G, H, K and L) and *Vangl2*^{+/*Lp*} embryos. Inset in C and D are transverse sections of *Vangl2*^{*Lp/Lp*} embryos. (E-H) Transverse section of embryos treated with CytD or (I-L) Y-27632. (A, C, inset in C, E, G, I and K) Sections immunolabelled for β -catenin or (B, D, inset in D, F, H, J and L) ZO1. The asterisks in C, D, the inset in C, D and in E-L mark the cellular disturbances. Scale bars: (B) 50 μ m, also applies to A and C-H; (L) 50 μ m, also applies to I-K.

Figure S7

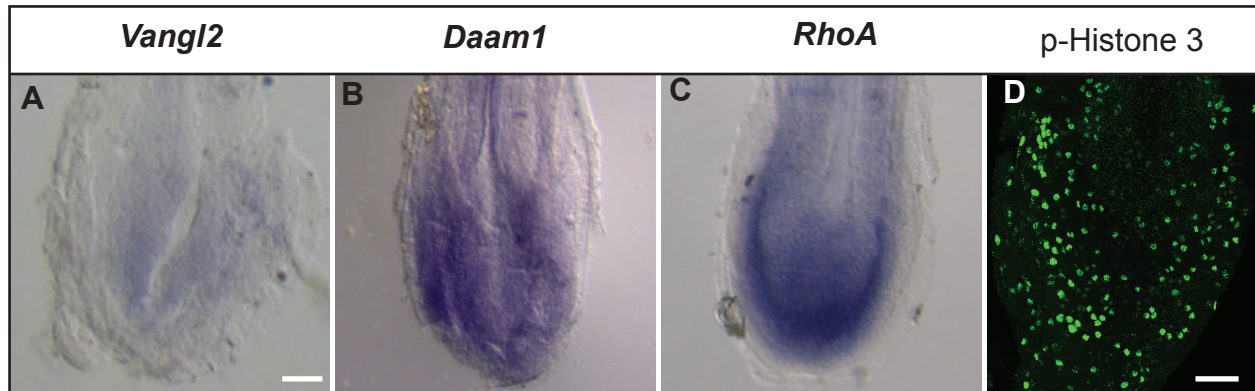


Figure S7: Wnt-PCP and proliferation in a dorsal view of the PNP. (A, B and C) Whole mount *in-situ* hybridisation of E9.5 mouse embryos showing *Vangl2* (A), *Daam1* (B) and *RhoA* (C) mRNA expression. (D) Whole mount immunolabelling for p-Histone 3. Scale bars: (A) 100 μm , also applies to B and C. (D) 50 μm .

Figure S8

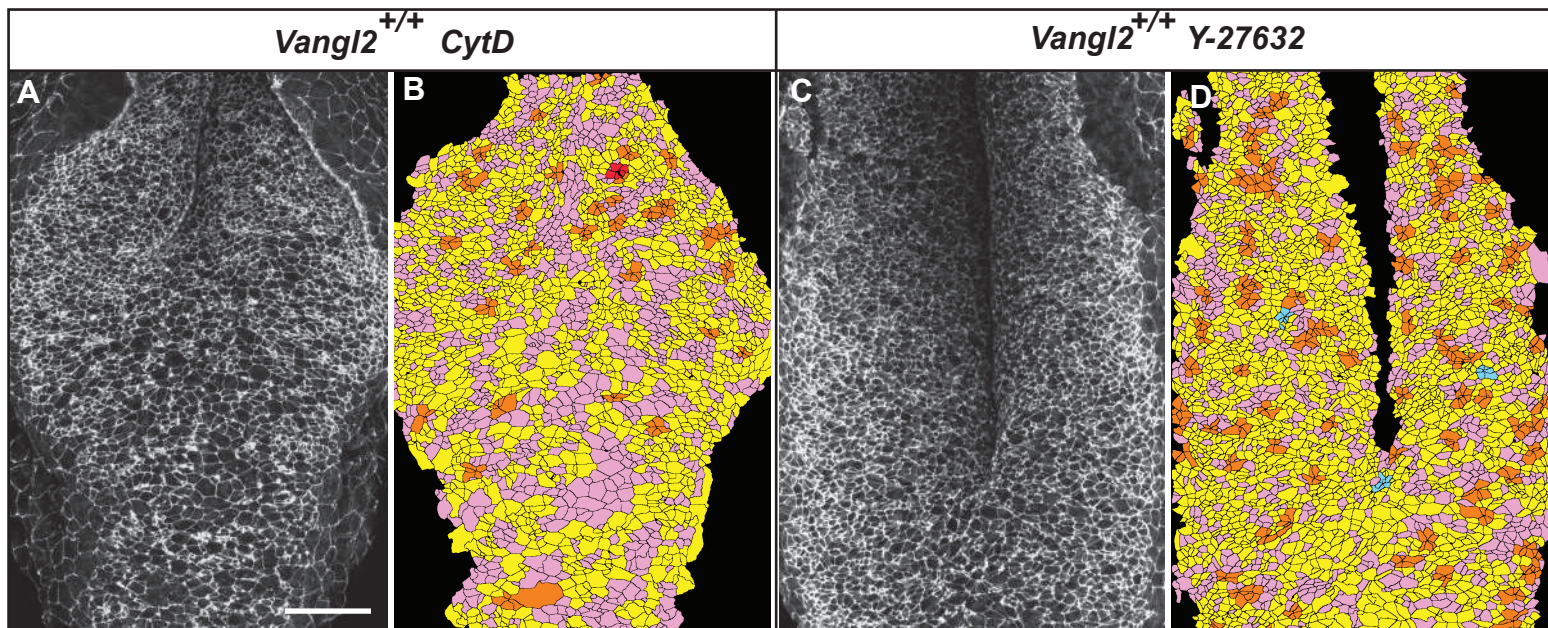


Figure S8: Altered apical cell constriction and cell reorganisation into rosettes at the PNP of *Vangl2*^{+/+} CytD and Y-27632 treated embryos. (A and B) Dorsal E9.5 PNP of *Vangl2*^{+/+} embryos treated with CytD or (C and D) Y-27632. (A and C) Embryos labelled for ZO1 and (B and D) segmented confocal images (Seedwater Segmenter) imported to Image J to define rosette formation. Rosette formation is represented in orange for cells with a vertex in a 5 cell rosette and blue for those in a 6 cell rosette. Cells that shared vertices with 4 or 3 cells were labelled in yellow and pink, respectively (not considered as rosettes). Scale bar: (A) 50 μ m also for B-D.

Figure S9

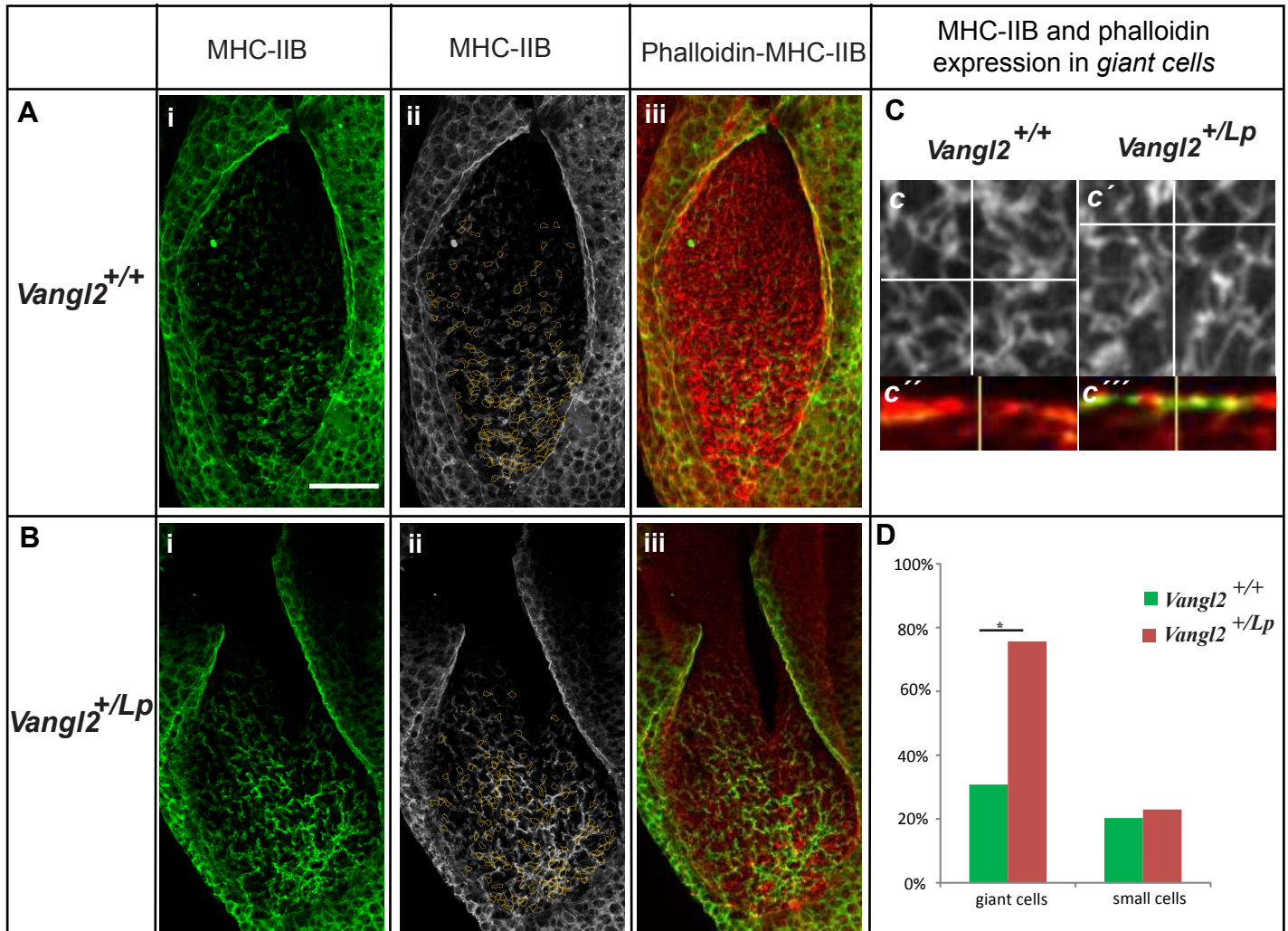


Figure S9: MHC-IIB expression in the *giant cell* population. (A) Dorsal view of a *Vangl2*^{+/+} and (B) *Vangl2*^{+/Lp} PNP showing the distribution of MHC-IIB (green in *i* and grey in *ii*) and of *giant cells* (outline in yellow in *ii*), and the merged MHC-IIB and phalloidin image (*iii*). (C) Amplification of the *giant cells* in *Vangl2*^{+/+} (*c*) and *Vangl2*^{+/Lp} (*c'*) embryos marked by the crossing point of the two axes and the corresponding orthogonal view (*c''* and *c'''*, respectively) MHC-IIB and phalloidin. (D) Graph representing the proportion of MHC-IIB positive *giant cells*, with significantly more MHC-IIB positive cells in the *Vangl2*^{+/Lp} than in the *Vangl2*^{+/+} ($p < 0.05$) embryos, as well as the MHC-IIB labelled *small cell* population. Scale bar in *Ai* 50 μ m, also applying to *Aii-iii*, *Bi-iii*.

Table S1:

	<i>Vangl2</i> ^{+/+}	<i>Vangl2</i> ^{+/<i>Lp</i>}
25-26 somites	12.5% (n=16)	12.5% (n=8)
27-28 somites	75% (n=12)	58.3% (n=12)
29-30 somites	100% (n=12)	86.6% (n=15)

Table S1: The tendency towards delayed NT closure in *Vangl2*^{+/*Lp*} embryos.

Percentage of closed neural tubes at different stages of development, in *Vangl2*^{+/+} and *Vangl2*^{+/*Lp*} embryos: n= number of embryos analysed.

Table S2:

	control	CytD	Y-27632
<i>Vangl2</i> ^{+/+}	5.01 $\mu\text{m}^2 \pm 0.162$	15.21 $\mu\text{m}^2 \pm 0.86^{**}$ (x 3)	8.20 $\mu\text{m}^2 \pm 0.34^{**}$ (x 1.64)
<i>Vangl2</i> ^{+/<i>Lp</i>}	7.21 $\mu\text{m}^2 \pm 0.3^{**}$ (x 1.44)	13.93 $\mu\text{m}^2 \pm 0.78^{**}$ (x 2.8)	9.31 $\mu\text{m}^2 \pm 0.43^{**}$ (x 1.85)
<i>Vangl2</i> ^{<i>Lp</i>/+<i>Lp</i>}	11.86 $\mu\text{m}^2 \pm 0.43^{**}$ (x 2.3)		

Table S2. Apical cell area in the cells in the region of the closing neural fold.

Average apical cell area (in $\mu\text{m}^2 \pm \text{SEM}$) in *Vangl2*^{+/+}, *Vangl2*^{+/*Lp*}, *Vangl2*^{*Lp*/*Lp*}, Cytochalasin D (CytD) and Y-27632 treated embryos. The increase in the apical cell area in *Vangl2*^{+/*Lp*}, *Vangl2*^{*Lp*/*Lp*}, and *Vangl2*^{+/+} Cytochalasin D (CytD) and Y-27632 treated embryos compared to *Vangl2*^{+/+} is indicated in brackets (n=3-4 embryos/condition). The number of cells analysed for each condition were: *Vangl2*^{+/+}, 141 cells; *Vangl2*^{+/*Lp*}, 165 cells; *Vangl2*^{*Lp*/*Lp*}, 128 cells; *Vangl2*^{+/+} treated with CytD, 126; *Vangl2*^{+/*Lp*} treated with CytD, 117; *Vangl2*^{+/+} treated with Y-27632, 128; *Vangl2*^{+/*Lp*} treated with Y-27632, 110; (** $p < 0.001$, representing the significant difference in the average size of the apical cell area between *Vangl2*^{+/+} and the other six conditions).

Table S3:

		<i>Vangl2</i> ^{+/+}	<i>Vangl2</i> ^{+/<i>Lp</i>}	<i>Vangl2</i> ^{+/+} CytD	<i>Vangl2</i> ^{+/+} Y-27632
PNT	CVFR* (CZ and PZ)	16.6% (17.7% and 16.04%)	7.4% (8.7% [§] and 6.7% [§])	9.5% (10.3% and 9%)	13.5% (13.5% and 13.5%)
	Rosette complexity	11.8%	4.6%	9%	7%
	ACA+ x (μm^2) (CZ and PZ)	7.43 (7.3 [†] and 7.5 [†])	11 (10 and 11.5)	10.17	9.93
	ACA CVFR (μm^2) ++	6.28 [¥]	9.64	8.76	9.46
	ACA N- CVFR (μm^2)	7.65 [¥]	11.1	10.3	10
NSB/CLE	CVFR**, ***	8.1%	3.1%	7.3%	8.3%
	Rosette complexity	11,3%	----	5.7%	3.9%
	ACA (μm^2) x , xx	11.5	17.05	14.87	11.52

Table S3. Cell morphology in the developing PNP.

Significant differences were observed using the proportion comparison test when the data was compared from: the (*) *Vangl2*^{+/*Lp*}, *Vangl2*^{+/+} CytD and *Vangl2*^{+/+} Y-27632 treated embryos to the *Vangl2*^{+/+}; (**) the PNT to NSB/CLE for each condition and in (***) the *Vangl2*^{+/*Lp*} to the *Vangl2*^{+/+} embryos; and (§) CZ to the PZ in the PNT of the *Vangl2*^{+/*Lp*}.

Significant difference were observed using the Mann-Whitney U test when comparing: the apical cell area (ACA) from (**X**) PNT to NSB/CLE for each condition and (**XX**) the *Vangl2*^{+/*Lp*}, *Vangl2*^{+/+} CytD and *Vangl2*^{+/+} Y-27632 treated embryos to the *Vangl2*^{+/+}; (¥) the CVFR and the N-CVFR in *Vangl2*^{+/+} embryos; (+) the *Vangl2*^{+/*Lp*}, *Vangl2*^{+/+} CytD treated embryos and *Vangl2*^{+/+} Y-27632 treated embryos compared to the *Vangl2*^{+/+} embryos; (++) the *Vangl2*^{+/*Lp*}, *Vangl2*^{+/+} CytD treated embryos and *Vangl2*^{+/+} Y-27632 treated embryos compared to the *Vangl2*^{+/+} embryos. (†) No significant difference were evident between the ACA of the CZ to the PZ in the PNT of the *Vangl2*^{+/+} ($p=0.72$).

Posterior neuropore (PNP); preneuronal tube (PNT); sub-zones of the PNT: central zone (CZ) and peripheral zone (PZ); most caudal part of PNP (NSB/CLE); cell with vertex forming a rosettes (CVFR); cells with no vertex forming rosettes (N-CVFR); percentage of high order rosettes (Rosette complexity); apical cell area (ACA, μm^2).

Table S4:

	genotype		T ⁺ /Sox2 ⁺	T ⁺ /Sox2 ⁻	T ⁻ /Sox2 ⁺	T ⁻ /Sox2 ⁻
General population cells in the PNT	<i>Vangl2</i> ^{+/+}	n=1272	82%	8.09%	5.66%	4.4%
	<i>Vangl2</i> ^{+/<i>Lp</i>}	n=1543	82.11%*	7.3%	5.2%**	5.4%
	<i>Vangl2</i> ^{+/+}	ACA (μm ²)	4.17‡	2.67‡	3.33‡	2.66
	<i>Vangl2</i> ^{+/<i>Lp</i>}	ACA (μm ²)	5.27‡	3.81‡	4.2‡	3.3
	<i>Vangl2</i> ^{+/<i>Lp</i>} vs <i>Vangl2</i> ^{+/+}	% ACA increase	126%	143%	126.6%	124%
Giant cells in the PNT	<i>Vangl2</i> ^{+/+}	n= 182	78%	9.4%	4.2% ⁺	8.4%
	<i>Vangl2</i> ^{+/<i>Lp</i>}	n= 578	71.5%*	9.3%	9.2% ^{+/**}	10.2%

Table S4: Presence of each cell type in the PNT and their apical cell areas in *Vangl2*^{+/+} and *Vangl2*^{+/*Lp*} embryos. This table shows the cell types found in the general population of the PNT of 4 *Vangl2*^{+/+} and 4 *Vangl2*^{+/*Lp*} embryos according to the expression of the *T* and *Sox2* genes, as well as in the “giant cell” population: neuromesodermal progenitors (T⁺/Sox2⁺); mesodermal cell (T⁺/Sox2⁻); neural cell (T⁻/Sox2⁺); unidentified cells (T⁻/Sox2⁻); the apical cell area (ACA) is given in μm²; n= number of cells analysed in each condition; the % ACA increase is the percentage increase in apical cell area between the *Vangl2*^{+/+} and *Vangl2*^{+/*Lp*} embryos for each type of cell.

(*). Significant difference between the percentages of T⁺/Sox2⁺ in the *giant cell* population compared to the general population of the PNT in *Vangl2*^{+/*Lp*} embryos ($p < 0.05$).

(**). Significant difference between the percentages of T⁻/Sox2⁺ in the *giant cell* population compared to the general population of the PNT in *Vangl2*^{+/*Lp*} embryos ($p < 0.05$).

(+), Significant difference when comparing the percentage of T⁻/Sox2⁺ in the “giant cell” population of the PNT of *Vangl2*^{+/+} vs *Vangl2*^{+/*Lp*} embryos ($p < 0.05$).

‡, Significant difference when comparing the apical cell area of the NMPs (T⁺/Sox2⁺) vs the mesodermal (T⁺/Sox2⁻) or neural cell fates (T⁻/Sox2⁺) for each genotype (Anova 1 factor with the *post-hoc* Games-Howell test, $p < 0.05$).

Table S5. Primers used for RT-QPCR.

Primer name	Reference	
GAPDH	(Rai et al., 2010)	
Wnt5a	(Hayashi et al., 2009)	
Prickle1	(Okuda et al., 2007)	
Glypican4	(Liu et al., 2014)	
Daam1	(Lopez-Escobar et al., 2015)	
β -actin	(Bolze et al., 2013)	
Myosin II-B	(Badirou et al., 2014)	
RhoA	(Chen et al., 2006)	
Primer name	Fw 5'-3'	Rv 5'-3'
PTK7	CAGTTCCTGAGGATTTCCAAGAA	AACACAGGGCCACCTTC
Shroom3	AAAGCCTTAGACATCACCGC	CAGAGACACTGTAGTAGGC

Table S6. Primary and secondary antibodies used.

Primary Antibodies	Source	Dilution	Reference
ZO1	Rabbit	1:150	40-2200 Invitrogen
ZO1	Goat	1:50	ab190085, Abcam
β -catenin	Mouse	1:200	610153 BD-bioscience
T	Goat	1:100	AF2085 R&D systems
Sox2	Mouse	1:100	MAB2018 R&D systems
Phosphor histone H3	Rabbit	1:500	06-570, Upstate Biotechnology
N-Cadherin	Mouse	1:100	18-0224 Invitrogen
Nonmuscle Myosin Heavy Chain II-B	Rabbit	1:150	PRB-445P Covance
Phospho-Myosin light chain 2 (Thr18/Ser19)	Rabbit	1:150	3674 Cell Signaling
Secondary antibodies			
anti-rabbit FITC conjugated	Goat	1:250	ab6717 Abcam
anti-mouse CyTM3 conjugated IgG	Goat	1:300	115-165-166 Jackson ImmunoResearch
Anti-goat FITC conjugated	Rabbit	1:50	61-1611, Invitrogen
anti-mouse alexa fluor 488 conjugated	Donkey	1:1000	A21202, Invitrogen
Donkey anti-rabbit alexa fluor 568 conjugated	Donkey	1:500	A10042, Invitrogen
Donkey anti-goat alexa fluor 633 conjugated	Donkey	1:800	A21082, Invitrogen

Table S7. Supplementary summary statistics

A) Power and size effect for the statistical significant data:

Reference	n	Study	<i>p</i>	D Cohen	Confidence interval	Power
Fig S3C Length	Wt=16 Het=16	(1)	0.013	1.8	0.95:2.6	91%
V-width	Wt=16 Het=16	(1)	0.04	0.8	-0.2:1.8	29.4%
L-V ratio	Wt=16 Het=16	(1)	<0.001	2.1	0.9:3.4	98.2%
Fig S4 Ectopic bending	Wt=14 Het= 20 CytD=14 Y-27= 10	(1)	<0.001 <0.001 <0.001	2.9 2.5 2.5	1.9:3.8 1.5:3.5 1.4:3.5	100% 98% 100%
Fig S5C mean value Actin intensity	Wt=120000 Het= 200000	(2)	<0.001	0.6	0.61-0.65	100%
Fig 2S N° cell alignments	Wt= 5 Het=11	(1)	0.001	2.6	1.22:4	91.9%
Fig 2U Cumuli	Wt=60 Het=60	(1)	<0.001	2.5	1.8:3.2	100%
Basal actin	Wt=60 Het=60	1)	0.06	0.3	-0.16:0.8	26.3%
Fig 2V N° cumuli	Wt=5 Het=8	(1)	0.15	0.8	-0.4:1.9	5.2%
Fig 4E Table S2 (**)	Wt=140 Het= 165 Hom=127 Wt-CytD=125 Het -CytD=116 Wt-Y-27=127 Het-Y-27= 109	(3)	<0.001	0.7 1.9 1.5 0.8 0.9 1.3	0.47:0.9 1.6:2.1 1.23:1.77 1.24:1.8 0.6:1.1 1:1.52	99.7% 100% 100% 100% 99.8% 100%
ACA CZ y PZ wt Table S3 (‡)	CZ=2422 PZ=4795	(2)	0,72	0.02	-0.02;0.07	100%
ACA CVFR vs N-CVFR Wt Table S3 (¥)	CVFR=1194 N-CVFR=6008	(2)	<0.001	0,2	0,16-0,28	82%
ACA PNT-PNT Table S3 (+)	Wt=7202 Het=5009 Wt=7202 Wt-cytD=5024 Wt=7202 Wt-Y-27=4866	(2) (2) (2) (2)	<0.001 <0.001 <0.001	0.5 0.4 0.3	0.45:0.52 0.33:0.4 0.3:0.37	100% 100% 100%
Apical size CVFR PNT Table S3 (++)	Wt=1194 Het=371 Wt=1194 Wt-cytD=475 Wt=1194 Wt-Y-27=472	(2) (2) (2) (2)	<0.001 <0.001 <0.001	0.5 0.3 0.4	0.37:0.6 0.24:0.45 0.34:0.5	100% 100% 100%
ACA PNT- CLE Table S3 (X)	Wt PNT=7202 CLE=2062 Het PNT=5000 CLE=958 CytD PNT=5024 CLE=1442 Y-27632 PNT=4866 CLE=1827	(2) (2) (2) (2)	<0.001 <0.001 <0.001	0.6 0.6 0.5 0,5	0.5-0.6 0.5-0.6 0.4-0.5 0.4-0.5	100% 100% 100% 100%
ACA Table S3 CLE-CLE (XX)	Wt=2062 Het=958 Wt=2062 Wt-cytD=1442 Wt=2062 Wt-Y-27=1827	(2) (2) (2)	<0.001 <0.001 <0.001	0.5 0.3 0.3	0.4-0.5 0.2-0.3 0.2-0.3	100% 99.7% 100%
Fig 6G Distance between p-myo paired cumuli (*)	Wt=188 Het= 248	(1)	<0.001	0.8	0,67-1,06	100%

B) Proportion comparison analysis:

reference	n	p	test	OR	Confidence interval	Power
Fig S5C % pixels with Max. value	Wt=220/120000 Het= 6/200000	<0.001	Chi-sq	61	27.2-137.8	100%
Fig 2R % alignments ML/AP	Wt=0/24 Het=4/15	0,03	Fisher Exact	0	0	-
% CVFR PNT-NSB/CLE Table S3 (**)	Wt PNT=1195/7202 CLE=167/2062	<0.001	Chi-sq	2,26	1.9:2.6	100%
	Het PNT=372/5000 CLE=30/958	<0.001	Chi-sq	2.5	1.7:3.6	99%
	CytD PNT=476/5024 CLE=105/1442	0.005	Chi-sq	1.33	1.07:1.66	66%
	Y-27 PNT=687/4866 CLE=153/1828	<0.001	Chi-sq	1.7	1.42:2.06	99.9%
% CVFR in wt CZ vs PZ Table S3	CZ=428/2426 PZ=769/4796	0,044	Chi-sq	1,1	0.9-1.2	17%
% CVFR PNT-PNT Table S3 (*)	Wt =1195/7202 Het=372/5000	<0.001	Chi-sq	2.47	2.19:2.8	100%
	Wt =1195/7202 CytD=476/5024	<0.001	Chi-sq	1.9	1.7:2.13	100%
	Wt=1195/7203 Y-27=687/4866	<0.001	Chi-sq	1.27	1.15:1.41	95.2%
% CVFR het CZ vs PZ Table S3 (§)	CZ=145/1647 PZ=228/3355	0,006	Chi-sq	1.32	1.07:1.64	54.5%
% CVFR NSB/CLE-NSB/CLE Table S3(***)	Wt =167/2062 Het=30/958	<0.001	Chi-sq	2.73	1.84:4.05	99.7%
	Wt =167/2062 CytD=105/1443	0.20	Chi-sq	1.1	0.87:1.4	9.7%
	Wt= 167/2062 Y-27=153/1827	0.37	Chi-sq	1.03	0.8:1.3	3.6%
Fig S9D Giant cells Small cells	Wt=49/159 Het=153/202	<0.001	Chi-sq	7	4.4-11.7	100%
	Wt=395/1947 Het=563/2451	0,016	Chi-sq	1,17	1.01-1.3	29,3%
Table S4 T ⁺ /Sox2 ⁺ Het GP/GC (*)	Het GP=1268/1543 GC=413/578	<0.001	Chi-sq	1.8	1.5-2.3	78.2%
Table S4 T ⁺ /Sox2 ⁺ Het GP/GC (**)	Het GP=81/1543 GC=53/578	<0.0009	Chi-sq	1.8	1.27-2.6	43.2%
Table S4 T ⁺ /Sox2 ⁺ in GC Wt/Het (+)	Wt=8/182 Het=53/578	0,04	Chi-sq	2.2	1.02-4,7	26%

(1) Student-t test

(2) Mann-Whitney U test

(3) Global comparisons of the cellular apical area were evaluated using an ANOVA test attending to the Welch correction and multiple comparisons were analysed using the post hoc Games-Howell test.

The apical cell area in the PNT under each condition was also compared to that in *Vangl2*^{+/+} embryos to obtain the size effect and power after employing a Mann-Whitney U test.

D Cohen (Lenhard & Lenhard ,2016): from <0: adverse effect; 0-0.1 No effect; 0.2-0.4: small effect; 0.5-0.7: intermediate effect; 0.8- >1: large effect.

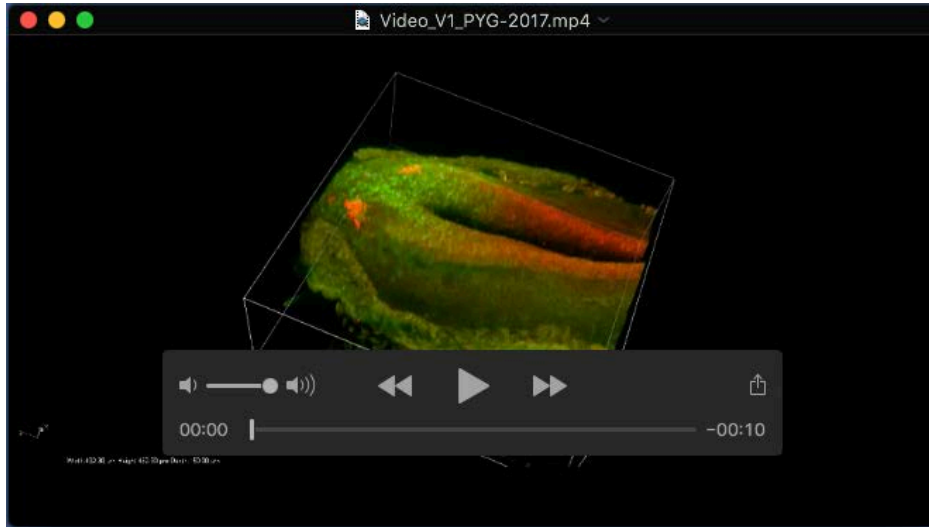
Power was calculated with Epidat software.

Chi-sq= Pearson's Chi-squared test.

Apical cell area (ACA).

General population (GC)

Giant cells (GC)



Movie 1

Sox2 and T distribution in the E 9.5 mouse embryo PNP.

3D reconstruction of the PNP: Sox 2 (labelled in red) marks early neural cells; T (labelled in green) marks early mesodermal cells. NMPs, bipotent progenitors co-express Sox2 and T (labelled in yellow).